Published in final edited form as:
Invest Ophthalmol Vis Sci. 2016 August 01; 57(10): 4498–4503. doi:10.1167/iovs.15-18362.

A Qualitative and Quantitative Assessment of Fundus Autofluorescence Patterns in Patients With Choroideremia

Jasleen K. Jolly[1,2,3], **Thomas L. Edwards**[1,2], **Jonathan Moules**[4], **Markus Groppe**[1], **Susan M. Downes**[1,2], and **Robert E. MacLaren**[1,2,3]

[1]Nuffield Laboratory of Ophthalmology, Department of Clinical Neurosciences, University of Oxford, Oxford Biomedical Research Centre, Oxford, United Kingdom

[2]Oxford Eye Hospital, John Radcliffe Hospital, Oxford, United Kingdom

[3]Moorfields Eye Hospital-UCL Institute of Ophthalmology, National Institute for Health Research Biomedical Research Centre, London, United Kingdom

[4]LightPear, Oxfordshire, United Kingdom

Abstract

Purpose—We set out to characterize the pattern of fundus autofluorescence (AF) loss in choroideremia (CHM) patients of varying ages and disease severity in order to determine the average rate of progression of this potential disease biomarker.

Methods—Fifty consecutive CHM patients (100 eyes) attending outpatient clinics at Oxford Eye Hospital underwent analysis with the Heidelberg OCT Spectralis with autofluorescence capabilities. The area of residual AF was traced using Heidelberg Eye Explorer. Bland-Altman analysis was used to calculate the coefficient of repeatability (CR). The degree of AF loss was correlated to different ages and the pattern of residual AF constructed into color-coded maps in order to gain insight into the mechanism of disease progression.

Results—The CR for measurement of AF area is <1%, indicating that a small change is likely to be significant. Correlation of patient age and area of residual AF produced a clinically relevant index of expected anatomic disease. Progression is 7.7% of the residual area each year (95% confidence intervals 7.0%–8.2%) and follows a logarithmic pattern with age ($r = 0.95$, $P < 0.001$). From this we derived the mean half-life of AF as 9 years. Qualitatively, the pattern of remaining AF centered on a point temporal to the fovea.

Conclusions—The area of residual AF in CHM can be measured reproducibly and shows a distinct pattern of loss. The measured residual area is inversely correlated to age. The ratio of the two variables may provide useful information regarding the rate of progression for any one individual at a given point in time.

Correspondence: Nuffield Laboratory of Ophthalmology, Levels 5 and 6 John Radcliffe Hospital West Wing, Headley Way, Headington, Oxford OX3 9DU, UK; enquiries@eye.ox.ac.uk.

Disclosure: **J.K. Jolly**, None; **T.L. Edwards**, None; **J. Moules**, None; **M. Groppe**, None; **S.M. Downes**, Novartis (R); **R.E. MacLaren**, NightstaRx Ltd, (S)

Europe PMC Funders Author Manuscripts

Keywords

choroideremia; fundus autofluorescence; quantification

Europe PMC Funders Author Manuscripts

Choroideremia (CHM) is a progressive X-linked inherited retinal degeneration affecting the retinal pigment epithelium (RPE), choroid, and outer retina. It is caused by defects in the *CHM* gene, which encodes Rab escort protein-1 (REP1), a key mediator of membrane trafficking in the retina and RPE. Early symptoms include nyctalopia and reduced peripheral vision followed by loss of visual acuity (VA) that may result in legal blindness as early as the third or fourth decade.1 With the advent of gene therapy as a possible treatment for CHM,2,3 it is important to establish reliable outcome measures for use in clinical trials, including objective measurements obtained by imaging.

Fundus autofluorescence (AF) is produced by retinoid byproducts of the visual cycle that accumulate in the RPE,4 and intensity has been reported to increase in healthy eyes with age.5 Although the majority of fundus AF originates from the RPE,6 photoreceptors have been shown to contribute to the AF signal.7,8 Autofluorescence imaging assists in the diagnosis of a wide range of retinal and RPE disorders, including age-related macular degeneration (AMD)9 and Stargardt disease,10 and can be a valuable independent marker of anatomic disease progression.11 Reduced AF signal is commonly associated with retinal dysfunction, as demonstrated by electrophysiology and perimetry studies12; for example, a decrease in signal corresponds to visual field loss in patients with retinitis pigmentosa and cone–rod dystrophies.13,14 An increase in signal tends not to accompany visual field loss13 but may be associated with a reduction in central vision.15

Choroideremia typically presents with a distinctive AF appearance.16 Choroideremia causes RPE degeneration, affecting the underlying choroid and overlying photoreceptors.1,17 Although the sequence of degeneration across the affected tissue layers has not been definitively established, there is growing evidence that loss of AF may precede significant retinal dysfunction.18 We collected AF data from a large number of patients with genetically confirmed CHM ($n = 50$) attending the outpatient clinics at Oxford Eye Hospital in order to (1) determine the test–retest repeatability of measuring the residual AF area for use in monitoring CHM; (2) correlate AF area loss with patient age, thus producing a standardized predicted rate of progression against which clinicians may compare their own patients; and (3) provide insights into the underlying anatomic changes occurring in eyes with CHM.

Methods

Patients were assessed as part of an ongoing CHM gene therapy clinical trial, approved by the research ethics committee (NCT01461213) and conducted in accordance with the Declaration of Helsinki 2013. Fundus autofluorescence images were collected from 100 eyes of 50 consecutive male patients with CHM seen in the ophthalmology outpatient clinics of the Oxford Eye Hospital. Images were captured using the 30° and 55° lens following pupil dilation using a Heidelberg Spectralis confocal scanning laser ophthalmoscope (Heidelberg Engineering, Heidelberg, Germany) with an excitation filter of 488 nm in automatic real-time (ART) mode using a minimum average of 25 scans. Per our standard practice, small

adjustments were required for both patient and camera position between images to optimize image quality. This is particularly important given the significant photophobia experienced by many of our CHM patients during AF imaging. Since the precise measurement (in mm^2) from the Heidelberg Eye Explorer would be dependent on parameters such as axial length and magnification, we decided to use the percentage area remaining from the 55° images in order to encompass the full extent of degeneration; that is, the total area of retinal islands was divided by the total area of the fundal image, generating an estimation of the percentage of remaining retina. This allowed standardized analysis of images across a cohort. These were converted back to area measurements (in mm^2) using the Heidelberg software for progression analysis in the clinical setting. Images were captured using standardized keratometry settings of 7.70 mm for each eye.

Two comparable but different images were taken on a single visit by the same photographer and analyzed to assess the test–retest variability of AF area measurements. Bland-Altman analysis was conducted to calculate the coefficient of repeatability (CR).19 The area of the remaining island of retina was plotted against age in years. The gradient of this line was used to calculate the expected progression of disease for the average patient at any one given point in time—known as the Choroideremia Index.

In order to compare all the residual AF islands across the entire cohort, Heidelberg Eye Explorer software was first used to manually outline the perimeter of the remaining retinal islands ≥ 0.05 mm^2 on the images. Scleral reflectance was not traced. The same software was used to mark digitally the center of the disc and the anatomic position of the fovea. The outlined islands encompassed by the tracings were colored in blue. These marked images were then exported as TIFF files. This process is shown in Supplementary Figure S1, showing the ease of delineating the residual islands from the background scleral reflectance.

Geographic Information Systems (GIS) Extract Transform Load (ETL) software (FME; Safe Software, Inc., Vancouver, BC, Canada) was then used to combine all patients' data into a composite heat map comprising overlapping outlined residual AF regions of all 100 eyes. This was performed by first automatically converting the TIFF files into "shapefiles" (a GIS file format). The images were georeferenced ("georeferencing" is the GIS term for aligning images consistently with a known base) by ensuring that the fovea on each AF image was given coordinates of 0,0. The image was then scaled to place the center of the optic cup at a constant *x*-coordinate of 200 units. Following this, the image was then rotated around the central coordinates (0,0) to give the optic cup center marking a *y*-coordinate of 0, thus giving the optic cup final coordinates of 200,0 consistently in all images. Although it is appreciated that the fovea is inferior to the optic disc, this distance can vary with refractive status, and the direct linear distance at the 200,0 position provides consistent disc–fovea alignment for all images. Once an image had been georeferenced, areas of the TIFF that had been marked as blue during the markup stage were detected and extracted using FME, thus converting each outlined area into a polygon (a vector geometry that covers an area).

The polygons for all eyes were overlapped, grouped by eye, using the AreaOnAreaOverlapper function in FME. This function counted how many polygons were stacked at any given location. The resultant summed polygon sets, one for each eye, were

exported to separate shapefiles. The shapefiles were loaded into QGIS version 2.6 (open source GIS software), and styled such that the number of eyes contributing to the preserved areas of retina at any given location was color coded into a heat map with a key displaying the information.

Results

The age range of the patients seen was 16 to 73 years (mean age 41 years). One patient was of South Asian extraction; 49 were Caucasian. Confirmed mutations in the *CHM* gene were seen in all patients in the cohort. The mutations are shown in the Supplementary Table. A Bland-Altman analysis was performed to establish the test–retest variability of our method for measuring the area of retained AF as a percentage of the total area photographed on a 55° image (Fig. 1). The figure comprises a total of 18 eyes from nine patients. For the remaining 82 eyes, only one image of sufficient quality for analysis was available due to the high level of photophobia experienced by the patients during the AF imaging. The CR was 0.5% with limits of agreement −0.5 to 0.5%.

There appears to be a high concordance between right and left eyes as shown in Figure 2 with a coefficient of determination (r^2) of 0.90, meaning that 90% of the total variation in one eye can be predicted by the linear relationship between the AF areas of the right and left eyes. Furthermore, the line of equality falls within the 95% confidence interval of the line of best fit, suggesting relative symmetry of AF area between right and left eyes.

In CHM, centripetal loss of AF typically progresses steadily over a patient's lifetime. By analyzing a cohort comprising a range of ages, it is possible to predict the average rate and extent of AF area loss over time (Fig. 3). The worse and better eyes follow a very similar pattern and are not significantly different ($P = 0.21$, Mann-Whitney U test). An extra sum of squares F-test showed that nonlinear regression models for the better and worse eyes were not significantly different ($P = 0.269$); hence the preferred model was one curve for all data sets (see Fig. 4). The gradient of the line is the rate of residual retinal loss, which we have defined as the Choroideremia Index. Taking into account the log axes, the Choroideremia Index for the remaining retina can be defined as $\log y = (-0.04 * x) + 2.53$, where y represents the area of residual retina and x is age in years. More simply, average log area (mm^2) for a given age is 2.53 – age/25. Hence the average 25-year-old patient would have 34 mm^2 ($10^{1.53}$) of residual AF, reducing to 3.4 mm by the age of 50 ($10^{0.53}$) and 0.34 mm by 75 years ($10^{-0.47}$), equivalent to a 10-fold reduction every 25 years. From this we also get a half-life of 8.7 years (95% confidence interval 8.1– 9.5). From this, the predicted average rate of progression for a CHM patient can be calculated per year as 7.7% of the residual retinal area per year (95% confidence intervals 7.0%–8.2%). For simplicity, Table 1 provides a reference for the expected area of remaining retina within a 55° image for different ages as calculated using the Choroideremia Index equation. The statistical significance of the R value in Figure 4 was calculated by $t = r/\text{sqrt}[(1 - r^2)/N - 2)]$ and returned a significance of $P < 0.001$.

To investigate whether certain retinal regions were resilient or were prone to degeneration, a composite map (Fig. 5) was constructed by overlapping the residual AF islands of 50 CHM

patients (brought into register around the disc and fovea). A number of patterns were observed. Across the cohort of 100 eyes (50 right and 50 left), fewer than 5 eyes on each side had retained AF around the optic disc, whereas up to 40 eyes for each side had preservation of AF around the fovea. There was a steady decay in the number of eyes with more peripheral preservation at increasing distance from the fovea. The pattern of central retained AF tended to demonstrate relative conservation in the vertical meridian. Similarly, the temporal macula appeared more resilient than the nasal macula. There appeared to be a vertical demarcation line both nasal and temporal to the macula.

To compare whether there was a difference in AF preservation on the nasal side of the fovea versus the temporal side of the fovea, the number of eyes with preserved AF at a point 100 μm nasal to the fovea was compared to the number of eyes with preserved AF at a point 100 μm temporal to the fovea using ANOVA testing. This showed greater preservation of AF temporally ($P = 0.0012$), confirming that the AF shrinkage converged toward a point just temporal to the fovea rather than directly to it. Right and left eyes were symmetrical in the pattern of preservation of AF displayed ($P = 0.42$) as shown in Table 2; that is, intereye symmetry was displayed, but there was intraeye asymmetry with greater temporal preservation in both eyes.

Discussion

We have identified a reproducible method that could be used in the clinical setting for quantifying change in AF area in CHM, and we show that the residual area is inversely correlated with age. This may be of use in identifying patients who are undergoing a more rapid degeneration early in the disease process and may help in the assessment of AF as a biomarker for disease progression when gene therapy for this condition is being applied. The integrated functionality of the widely available Heidelberg Eye Explorer software can be a valuable tool for assessing AF images of CHM patients. The repeatability of our area method for quantifying residual AF (CR = <1%) was lower than that found using an alternative methodology based on quantification of AF gray levels,9 although the two approaches are not directly comparable, resulting in different repeatability measures. For example, the percentage area of residual AF did not include an adjustment for variability in disc size; that is, disc area was not subtracted from total AF area. While inclusion of this as an additional step may have changed the reproducibility of our methodology, we do not anticipate that this would influence serial percentage AF measurements over time. This decision was taken in order to facilitate the ease of routine application of this methodology in a clinical setting. Furthermore, these two methods may be complementary in the assessment of retinal degenerations, applying to different disease processes. For example, the area method relies on a well-defined border between normal and abnormal AF, for example, CHM, while the qAF method may be better suited to defining more graded transitions of grayscale levels, for example, Stargardt disease.

A number of factors can impact the reproducibility of AF image capture. Several factors can affect the intersession variability, such as changes in media opacities, centration of the images, and different personnel taking either the images or the measurements or both. Degradation of image quality can reduce the accuracy of AF area measurements, so it is

important that variables such as pupil diameter, image settings, image centration, focusing, and patient positioning19 be controlled during imaging. Pupil size is controlled for by maximal dilation using mydriatic drops prior to imaging. Standard operating procedures (SOPs) for imaging provide guidance for image acquisition, centration, optimization of focusing, ensuring a steady head, and gaze position. The presence of media opacity should also be noted. Media opacities decrease the intensity of an AF signal and increase its signal-to-noise ratio, which cannot currently be fully mitigated. However, because our method relies on identifying the border of residual AF, and not on the absolute level of AF itself, mild to moderate media opacity should have a limited impact provided that there was adequate luminance to demarcate the outline of surviving AF islands.4,20

Both 30° and 55° angles of image capture were used in this study. The optimal magnification for clinical application may depend on the stage of disease. For example, it may be helpful to use 55° images to monitor for progression in early stages of the disease and 30° images in more advanced cases of the disease. In earlier stages of the disease, the surviving area of retina extends beyond the borders of the 30° image, so subtle peripheral changes may be missed if one is not monitoring with the wider-angle lens. In later stages of the disease, when the islands are small, the increased magnification of the smaller field images should allow better visualization and more accurate measurement of the residual retinal islands.

We sought to investigate the relationship between age and residual retinal AF as a marker for the rate of disease progression. The Choroideremia Index calculates an expected residual AF for a given age, providing a useful indication of expected rate of progression for clinicians, visual scientists, and patients. Additionally, the Choroideremia Index may be beneficial in assessing the optimal time point at which to intervene with emerging treatments such as gene therapy.2 The log progression nature of the graph explains the greater loss of retina at a younger age, with slowing of the degeneration at later stages, when there is less retinal area remaining to lose. A simple reference table was provided for use in clinics, as the Choroideremia Index calculation has been performed for various ages as a guidance tool. The logarithmic relationship we have defined has also been noted in a recent study on CHM patients in Germany and hence may be widely applicable.21 Out of our 50 patients, 1 had a missense mutation, and 49 patients had a presumed null mutation. This is in agreement with a recent publication reporting that missense mutations are rare in CHM and that the mutation type does not impact genotype–phenotype correlation22 so is unlikely to impact the rate of disease progression.

In addition to quantifying residual AF area, the pattern of its loss can provide further insights into disease mechanisms. For example, choroicapillaris defects in geographic atrophy result in certain patterns of lobular AF loss, indicating a vascular component to the disease process.4 Furthermore, normalized AF luminance maps have been found to correspond to rod density within the retina in human donor eyes (Ach T, et al. *IOVS* 2015;56:ARVO E-Abstract 2370).8 This was supported by the observation that the spatial distribution of AF signal across the fundus was similar in Stargardt disease and healthy subjects. For both groups, the AF signal is highest superotemporally. At this position the rod density has been reported to be the highest.9

The pattern of AF preservation revealed a high degree of preservation of AF around the macula area, with relative preservation of AF in the temporal retina and greater loss of AF around the optic disc. One explanation for the discrepancy between nasal and temporal retinal involvement may also be the higher rod photoreceptor concentration in this area of the retina.8 The area of greatest preservation of AF was the fovea, which is a rod-free zone but has a similar high density of cone photoreceptors. When imaging technologies progress further to visualize rod cells in the human retina, it would be interesting to see if the spatial preservation of AF matches the areas of preservation in rod cells. The cone photoreceptors appear to do functionally better compared to rods in patients with CHM, as evidenced by the relative preservation of the VA until very late stages of the disease. It is therefore feasible that cone survival may contribute to RPE survival in areas with a higher cone density.

A further consideration is the relationship between RPE and melanin. The function of Rab27a protein is reduced by the lack of REP1. Rab27a is a retina-specific protein, thought to affect melanosome transport and localization in the RPE and choroid.23 Melanin content of RPE cells increases in the second decade of life, then proceeds to decline with age.24 This may explain why CHM mostly affects patients in their second decade and may also be related to the decreasing rate of degeneration as shown by the Choroideremia Index equation. The highest concentration of melanin is found in peripheral RPE cells, and loss over time is highly variable both centrally and peripherally.23 This may explain the variability of the exact areas of remaining retina, as no single area of preserved retina had the contribution of more than 40 eyes.

Another factor possibly affecting RPE survival may be the choroidal blood supply. The distribution of the choroidal blood vessels differs in the macula region, equatorially and peripherally.25 This fits with the pattern of maximum preservation of AF in the macula region, followed by preservation within the posterior pole, with greatest loss in the periphery. The choroidal blood supply is most dense in the center,26 less dense temporally, and even less dense nasally,27 potentially related to the earlier loss of AF found nasally if the choroicapillaris is thinner in this region. There do not appear to be any studies looking at inferior versus superior differences in choroidal blood supply. Regardless of the mechanism, the pattern of AF preservation is also useful in a clinical context. Patients can be advised of the expected pattern of loss, allowing low-vision rehabilitation services to provide more targeted support systems and advice.

In summary, we have shown that calculating residual AF area, expressed as a percentage of total image area, is a repeatable and useful outcome measure for assessing CHM. This may be of particular relevance in the context of an interventional clinical trial, where one might expect to see a slowing of the rate of AF loss over time. The Choroideremia Index provides clinicians with a simple tool for quickly assessing the extent of an individual patient’s progression as compared to the mean of a similar-aged cohort.

Supplementary Material

Refer to Web version on PubMed Central for supplementary material.

Acknowledgments

Supported by the National Institute for Health Research (NIHR) Oxford Biomedical Research Centre based at Oxford University Hospitals National Health Service Trust and University of Oxford, The Health Innovation Challenge Fund, Fight for Sight.

The views expressed are those of the authors and not necessarily those of the NHS, the NIHR, or the Department of Health. The sponsor and funding organization had no role in the design or conduct of this research.

References

1. MacDonald IM, Russell L, Chan C-C. Choroideremia: new findings from ocular pathology and review of recent literature. Surv Ophthalmol. 2009; 54:401–407. [PubMed: 19422966]
2. Maclaren RE, Groppe M, Barnard AR, et al. Retinal gene therapy in patients with choroideremia: initial findings from a phase 1/2 clinical trial. Lancet. 2014; 6736:1–9.
3. Edwards TL, Jolly JK, Groppe M, et al. Visual acuity after retinal gene therapy for choroideremia. N Engl J Med. 2016; 374:1996–1998. [PubMed: 27120491]
4. Schmitz-Valckenberg S, Holz FG, Bird AC, Spaide RF. Fundus autofluorescence imaging: review and perspectives. Retina. 2008; 28:385–409. [PubMed: 18327131]
5. Greenberg JP, Duncker T, Woods RL, et al. Quantitative fundus autofluorescence in healthy eyes. Invest Ophthalmol Vis Sci. 2013; 54:5684–5693. [PubMed: 23860757]
6. Von Rückmann A, Fitzke FW, Bird AC. Distribution of fundus autofluorescence with a scanning laser ophthalmoscope. Br J Ophthalmol. 1995; 79:407–412. [PubMed: 7612549]
7. Flynn E, Ueda K, Auran E, et al. Fundus autofluorescence and photoreceptor cell rosettes in mouse models. Invest Ophthalmol Vis Sci. 2014; 55:5643–5652. [PubMed: 25015357]
8. Ach T, Huisingh C, McGwin G, et al. Quantitative autofluorescence and cell density maps of the human retinal pigment epithelium. Invest Ophthalmol Vis Sci. 2014; 55:4832–4841. [PubMed: 25034602]
9. Fleckenstein M, Schmitz-Valckenberg S, Lindner M, et al. The “diffuse-trickling” fundus autofluorescence phenotype in geographic atrophy. Invest Ophthalmol Vis Sci. 2014; 55:2911–2920. [PubMed: 24699379]
10. Burke TR, Duncker T, Woods RL, et al. Quantitative fundus autofluorescence in recessive Stargardt disease. Invest Ophthalmol Vis Sci. 2014; 55:2841–2852. [PubMed: 24677105]
11. Delori F, Goger D, Dorey C. Age-related accumulation and spatial distribution of lipofuscin in RPE of normal subjects. Invest Ophthalmol Vis Sci. 2001; 42:1855–1866. [PubMed: 11431454]
12. Lois N, Halfyard AS, Bird AC, et al. Fundus autofluorescence in stargardt macular dystrophy-fundus flavimaculatus. Am J Ophthalmol. 2004; 138:55–63. [PubMed: 15234282]
13. Ogura S, Yasukawa T, Kato A, et al. Wide-field fundus autofluorescence imaging to evaluate retinal function in patients with retinitis pigmentosa. Am J Ophthalmol. 2014; 158:1093–1098. [PubMed: 25062603]
14. Oishi M, Oishi A, Ogino K, et al. Wide-field fundus autofluorescence abnormalities and visual function in patients with cone and cone-rod dystrophies. Invest Ophthalmol Vis Sci. 2014; 55:3572–3577. [PubMed: 24845635]
15. Oishi A, Ogino K, Makiyama Y, et al. Wide-field fundus autofluorescence imaging of retinitis pigmentosa. Ophthalmology. 2013; 120:1827–1834. [PubMed: 23631947]
16. Yuan A, Kaines A, Jain A, et al. Ultra-wide-field and autofluorescence imaging of choroidal dystrophies. Ophthalmic Surg Lasers Imaging. 2010; 41:e1–e5.
17. Tolmachova T, Wavre-Shapton ST, Barnard AR, et al. Retinal pigment epithelium defects accelerate photoreceptor degeneration in cell type-specific knockout mouse models of choroideremia. Invest Ophthalmol Vis Sci. 2010; 51:4913–4920. [PubMed: 20445111]
18. Edwards TL, Groppe M, Jolly JK, et al. Correlation of retinal structure and function in choroideremia carriers. Ophthalmology. 2015; 122:1274–1276. [PubMed: 25682176]
19. Bland JM, Altman D. Statistical methods for assessing agreement between two methods of clinical measurement. Lancet. 1986; 1:307–310. [PubMed: 2868172]

20. Issa PC, Singh MS, Lipinski DM, et al. Optimization of in vivo confocal autofluorescence imaging of the ocular fundus in mice and its application to models of human retinal degeneration. Invest Ophthalmol Vis Sci. 2012; 53:1066–1075. [PubMed: 22169101]
21. Seitz IP, Zhour A, Kohl S, et al. Multimodal assessment of choroideremia patients defines pre-treatment characteristics. Graefes Arch Clin Exp Ophthalmol. 2015; 12:2143–2150.
22. Feund PR, Sergeev YV, MacDonald IM. Analysis of a large choroideremia dataset does not suggest a preference for inclusion of certain genotypes in future trials of gene therapy. Mol Genet Genomic Med. 2016; 4:344–358. [PubMed: 27247961]
23. Hume AN, Collinson LM, Rapak A, et al. Rab27a regulates the peripheral distribution of melanosomes. J Cell Biol. 2001; 152:795–808. [PubMed: 11266470]
24. Feeney-Burns L, Hilderbrand ES, Eldridge S. Aging human RPE: morphometric analysis of macular, equatorial, and peripheral cells. Invest Ophthalmol Vis Sci. 1984; 25:195–200. [PubMed: 6698741]
25. Yoneya S, Tso MO. Angioarchitecture of the human choroid. Arch Ophthalmol. 1987; 105:681–687. [PubMed: 3619746]
26. McLeod DS, Lutty GA. High-resolution histologic analysis of the human choroidal vasculature. Invest Ophthalmol Vis Sci. 1994; 35:3799–3811. [PubMed: 7928177]
27. Choi W, Mohler KJ, Potsaid B, et al. Choriocapillaris and choroidal microvasculature imaging with ultrahigh speed OCT angiography. PLoS One. 2013; 8:e81499. [PubMed: 24349078]

Europe PMC Funders Author Manuscripts

Europe PMC Funders Author Manuscripts

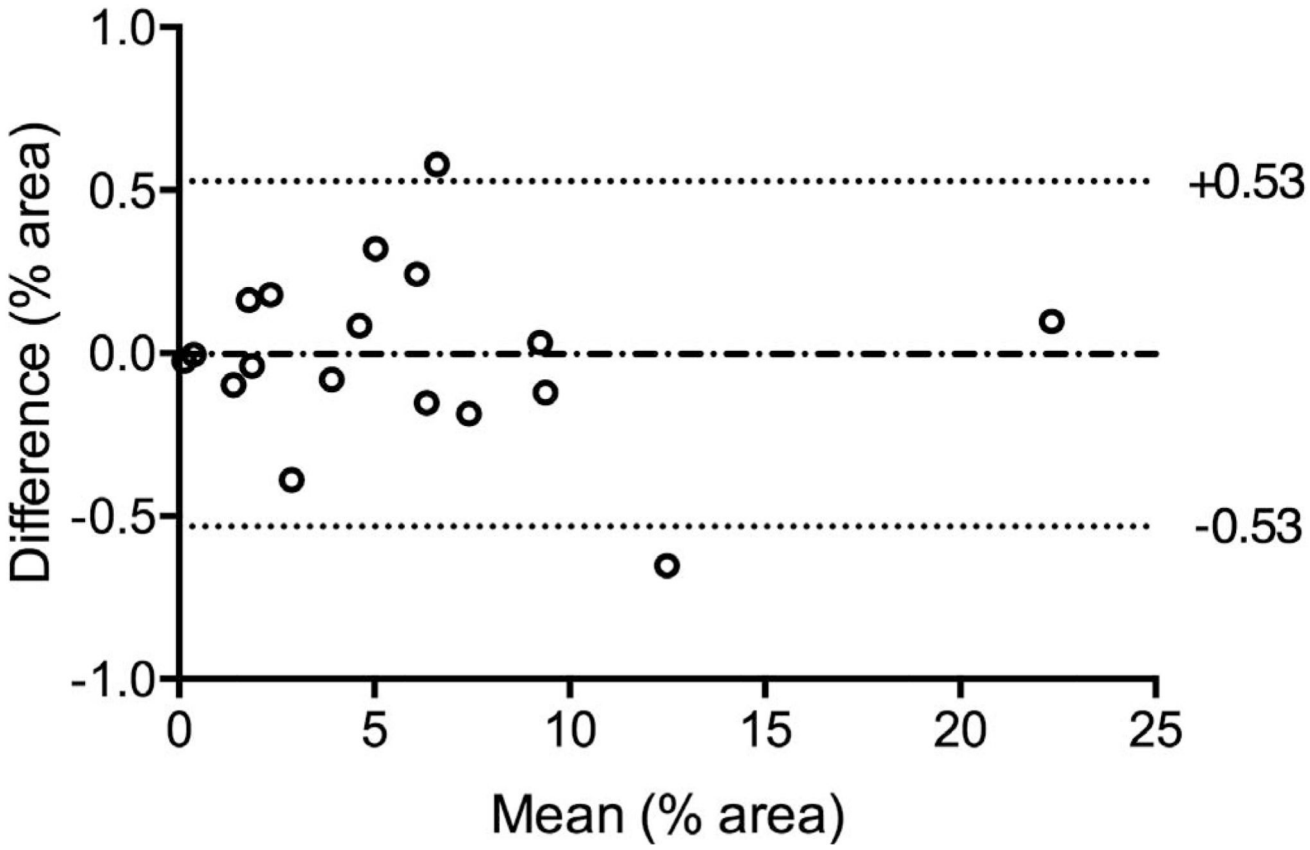

Figure 1.
Bland-Altman analysis for remaining retina based on percentages calculated from 55° autofluorescence (AF) images. *Dashed line* represents mean of differences and the *dotted lines* represent the limits on confidence.

Europe PMC Funders Author Manuscripts

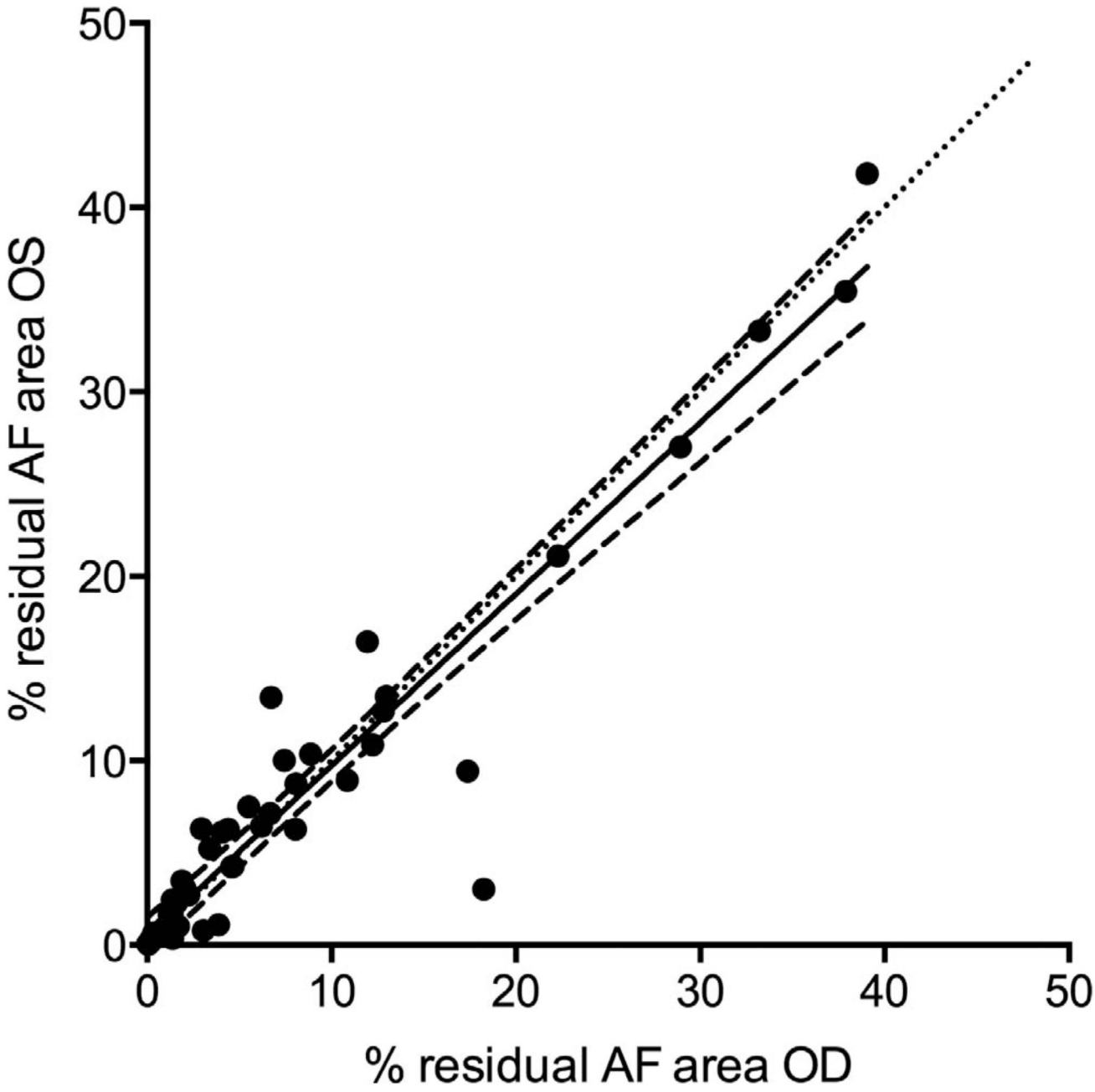

Figure 2.

Symmetry of residual AF (fundus autofluorescence) area as a percentage between right (OD) and left (OS) eyes. The *dashed lines* represent the 95% confidence intervals. The *dotted line* represents the line of equality. The *solid line* is the best fit to the data.

Europe PMC Funders Author Manuscripts

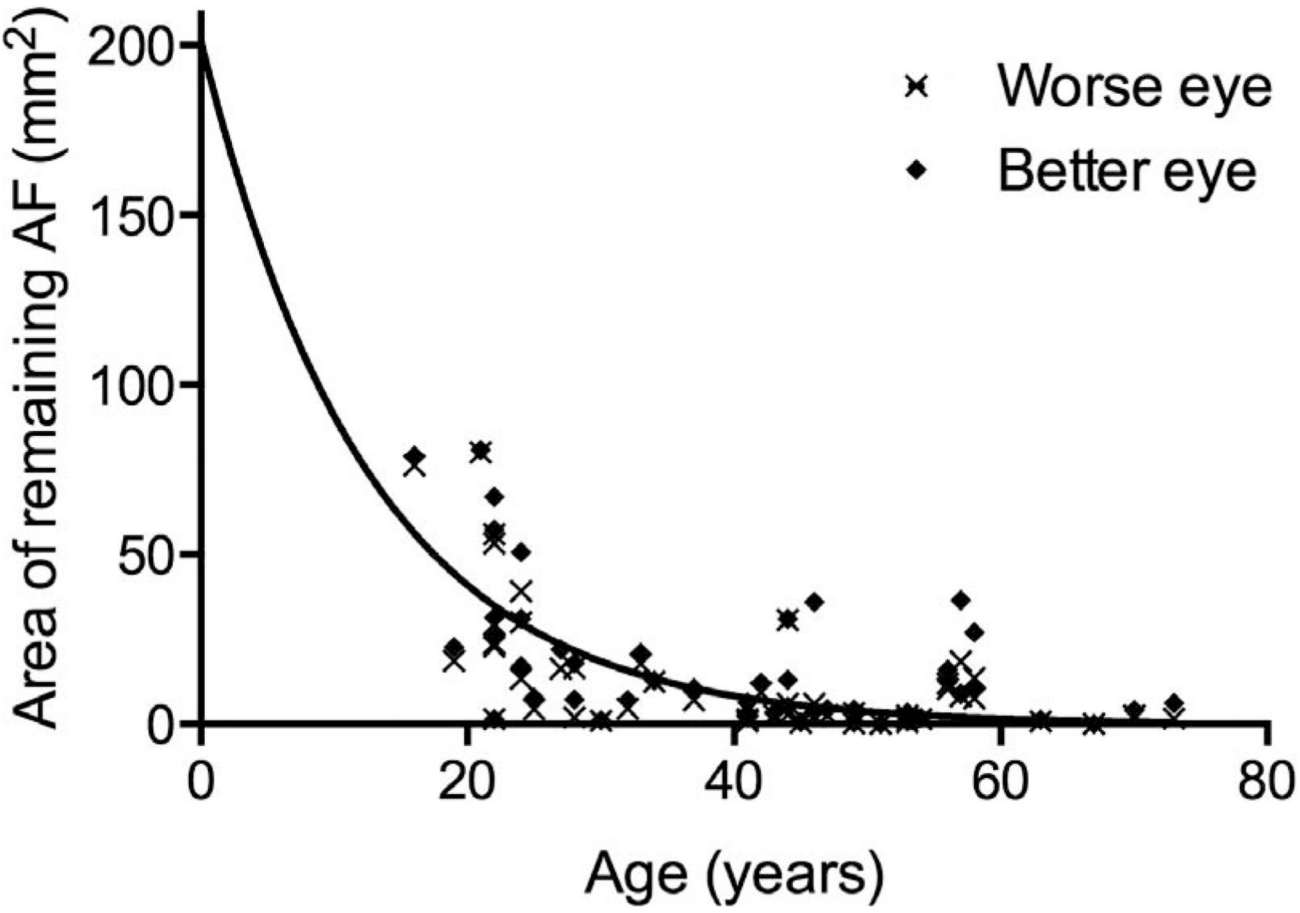

Figure 3.

Effect of age on AF (fundus autofluorescence) area plotted on linear axes. The better and worse eyes (in terms of AF area when compared to each other in each patient) are indicated by the key and follow the same curve with increasing age, $n = 50$ patients. The y-intercept was constrained by the mean maximal area that could be imaged using the equipment with the mean disc area subtracted (201.4 mm^2).

Europe PMC Funders Author Manuscripts

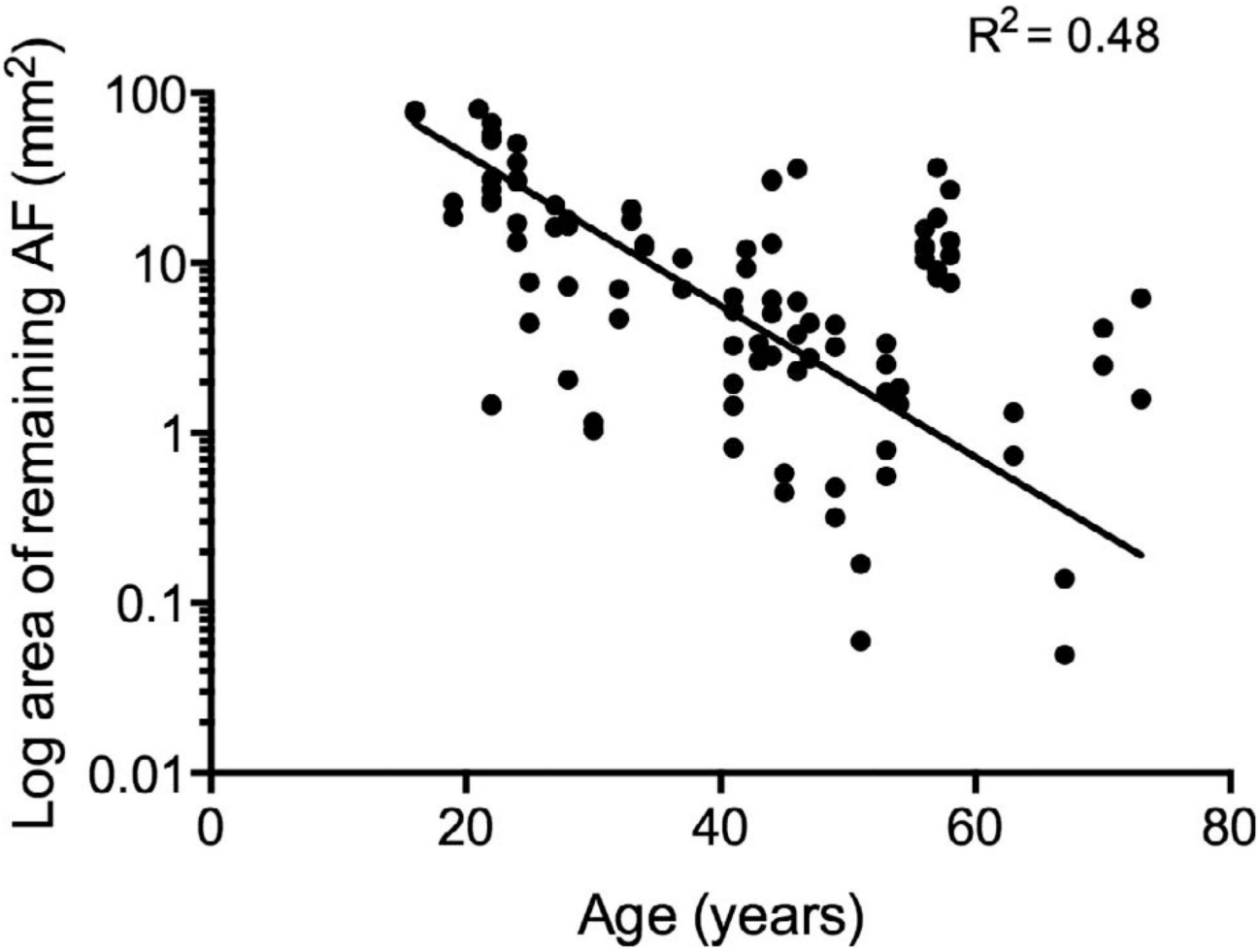

Figure 4.

Choroideremia Index calculation for remaining retinal area in eyes with choroideremia. Age is plotted on a linear scale and area on a log scale due to the logarithmic nature of the relationship. The equation defines the Choroideremia Index and shows the relationship between remaining retina and age. Taking into account the log axes, the Choroideremia Index for the remaining retina can be defined as (log area - 2.53)/age. In other words, the expected log area for any age can be calculated by (−0.04 * age) + 2.53.

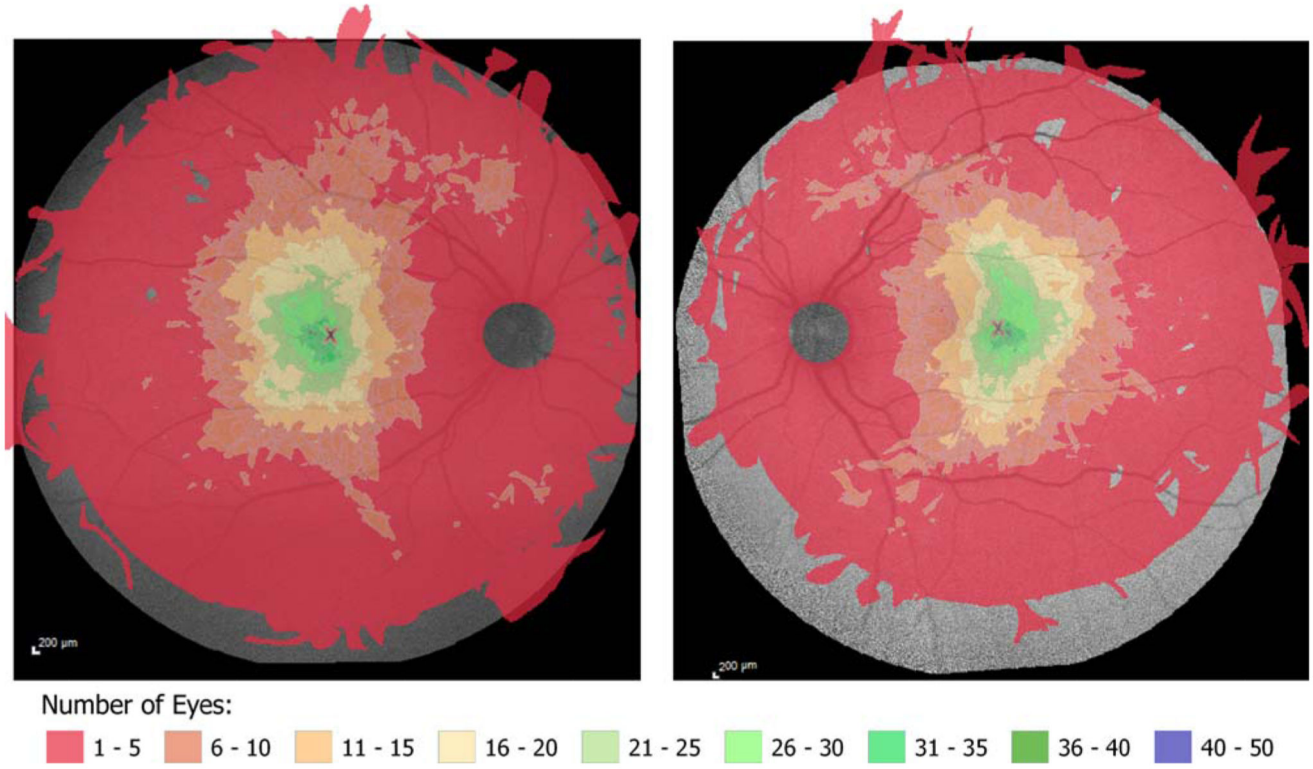

Figure 5.

Map of AF (fundus autofluorescence) preservation. A composite heat map image of the right eyes is presented on the *left*, and a composite heat map image of the left eyes is presented on the *right* per clinical convention in order to represent areas of residual retina in choroideremia.

Europe PMC Funders Author Manuscripts

Europe PMC Funders Author Manuscripts

Table 1

Choroideremia Index Table for Expected Remaining AF Area Based on Age as Calculated From the Regression Line Based on Data From 100 Eyes With Choroideremia

Age, Years	Expected Retinal Area Remaining, mm^2	Age, Years	Expected Retinal Area Remaining, mm^2
20	54	42	7.1
22	45	44	5.9
24	37	46	4.9
26	31	48	4.1
28	26	50	3.4
30	21	52	2.8
32	18	54	2.3
34	15	56	1.9
36	12	58	1.6
38	10	60	1.4
40	9	62	1.1

Europe PMC Funders Author Manuscripts

Table 2

The Presence or Absence of AF at the Fovea, and at Two Points Along the Horizontal Meridian (100 μm Nasal and 100 μm Temporal to the Fovea), Was Documented in 50 Eyes of 50 Patients; Table Shows Those Eyes With Preserved AF at These Locations

Eye	Nasal	Central	Temporal
OD	16	31	28
OS	15	31	28